Summary results of 2019 ICOLD Benchmark Workshop on seismic analysis of Pine Flat Dam

J.W. Salamon and C. Wood
U.S. Bureau of Reclamation, USA

M.A. Hariri Ardebili
University of Colorado at Boulder, USA

R. Malm
KTH Royal Institute of Technology, Sweden

G. Faggiani
Ricerca sul Sistema Energetico - RSE S.p.A., Italy

ABSTRACT:

The ICOLD Committee on Computational Aspects of Analysis and Design of Dams organized the 15th International Benchmark Workshop on Numerical Analysis of Dams on September 9-11, 2019 in Milan, Italy. Theme A of the workshop was related to seismic analyses of Pine Flat Dam. In the benchmark study, 32 contributions were submitted for six study cases that included simulating an eccentric-mass vibration generator test conducted at Pine Flat Dam in 1971, assessing model uncertainties arising from applying various types of the free-field boundary condition to foundation using impulsive load excitations, assessing the influence of reservoir level on the response of a dam to seismic loads, assessing alternative approaches to nonlinear analysis of concrete dams, and performing a comparison analysis for the models with mass and massless foundations.

In this paper, the benchmark study cases are presented together with selected analysis results and general conclusions. A need for developing best practices for advanced analyses of concrete dams is also discussed.

INTRODUCTION

1.1 *General*

The case studies of the ICOLD Committee's 15th International Benchmark Workshop continue the investigations initiated by the United States Society on Dams (USSD) Concrete Dams Committee and Earthquakes Committee during the workshop organized during the 2018 USSD Annual Conference and Exhibition in Miami, Florida, on May 3, 2018, titled, "*Evaluation of Numerical Models and Input Parameters in the Analysis of Concrete Dams*" (Bureau of Reclamation, 2018). The purpose of these workshops is to investigate uncertainties in numerical analyses of concrete dams using a focused, systematic, and controlled approach with collaborative participation from the international dam industry and academia.

The Formulation Committee (Formulators) for ICOLD Theme A benchmark have defined new study cases for a model of Pine Flat Dam (Salamon et. al, 2019) based on the outcomes from the previous USSD 2018 workshop. The goals of this new study are to identify key uncertainties that may significantly affect numerical modeling of concrete dams, determine research needs, and develop best practices in the advanced analysis of concrete dams.

The objective of this effort is to begin developing such a framework by examining how complex problems might be divided into simpler subproblems that have tractable solutions. Development of this framework is expected to benefit the profession by establishing a common conceptual basis for the advanced seismic analysis of concrete dams.

The formulated study cases are intentionally narrow in focus in order to identify the assumptions, analysis parameters, and methods having the greatest effect. Simple model geometry and analysis input parameters are defined in the formulations to avoid overtaxing workshop contributors (Contributors), but which, in aggregate, will produce meaningful results from the work submitted by each Contributor.

Overall, 28 Contributors participated in the Theme A benchmark workshop in Milan (8 from universities and 20 from consulting and government). Some Contributors provided more than one solution. A large dataset of results has been collected and processed by the Formulators. A summary of the preliminary results, available at: https://www.itcold.it/relazioni-e-atti/, was presented during the

workshop in Milan (ICOLD, 2019). The full set of the results, summary, and conclusions, together with the Contributor's papers, will be included in the final workshop proceeding.

1.2 *Conceptual model*

The Theme A study includes analyses of the tallest nonoverflow Pine Flat Dam monolith. The "*base configuration*" of the model is defined as shown in Figure 1. The foundation dimensions (Figure 1) are: length: H-G = 700 m, depth: I-H = 122 m, dam heel location: I-A = 305 m, and reservoir water level: 268.21 m.

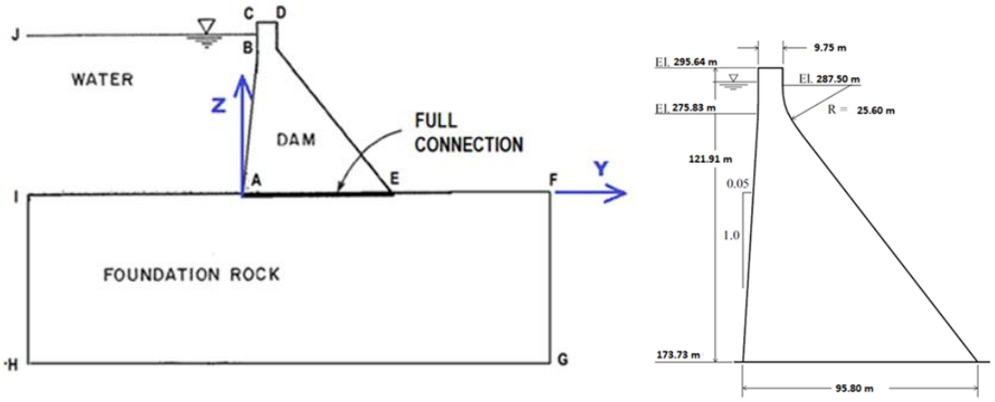

Figure 1. Base configuration for the Pine Flat Dam model of Monolith 16.

The same elastic properties were assumed for concrete and foundation materials: elastic modulus of 22,410 MPa, density of 2,483 kg/m^3, and Poisson's ratio of 0.2. Gravity and hydrostatic loads, together with various seismic excitations records, were defined in the formulation together with the defined viscous damping parameters.

The boundary conditions at the bottom, upstream, and downstream faces of the foundation block were selected by the Contributors.

1.3 *Purpose of studies*

Particular interests of the benchmark studies included the quantitative evaluation of various boundary conditions, the effect of foundation block sizes in seismic wave simulation, the influence of the reservoir water levels on the response of the dam structure, the validation of the analysis models with mass and massless foundation, and the nonlinear behavior of concrete dams.

Six case studies were proposed by Formulators. Each one intends to capture a specific feature of numerical simulation of the dam-reservoir-foundation system. The case study descriptions and selected analysis results are presented below.

2 CASE STUDIES AND ANALYSIS RESULTS

2.1 *Case A – EMVG simulation*

The purpose of Case A was to allow Contributors to validate their models against experimental results before continuing the analysis with the more advanced cases. For this purpose, Contributors were asked to determine the six natural frequencies and the corresponding mode shapes for the dam-foundation-reservoir system (the base model) and conduct simulation of a field testing performed at Pine Flat Dam in 1971 (Rea, Liaw & Chopra, 1972).

In total, 23 teams submitted results. In general, the natural frequencies and mode shapes corresponded well with the field measurements, see Figure 2. For instance, the median frequency obtained from all Contributions matched the result of the first fundamental frequency of 3.47 Hz from the experiments. The mean for this frequency was 3.53 Hz with a standard deviation of 0.46 Hz. Compared to the experiments, it was apparent that several natural frequencies were obtained in the numerical models that could not be identified in the experiments. Some Contributors also included non-structural modes, which may be a reason for the discrepancy between the results. This can be seen in the top left figure where two Contributors obtained the first natural frequency for a non-structural mode at 1.5 Hz, which offsets their results for the remaining modes. One additional observation is

that the measurements clearly show 3D behaviour of the whole dam, which is difficult to interpret from a finite element (FE) analyses of a single monolith. An example of this is shown for the natural frequency of 3.47 Hz in Figure 2.

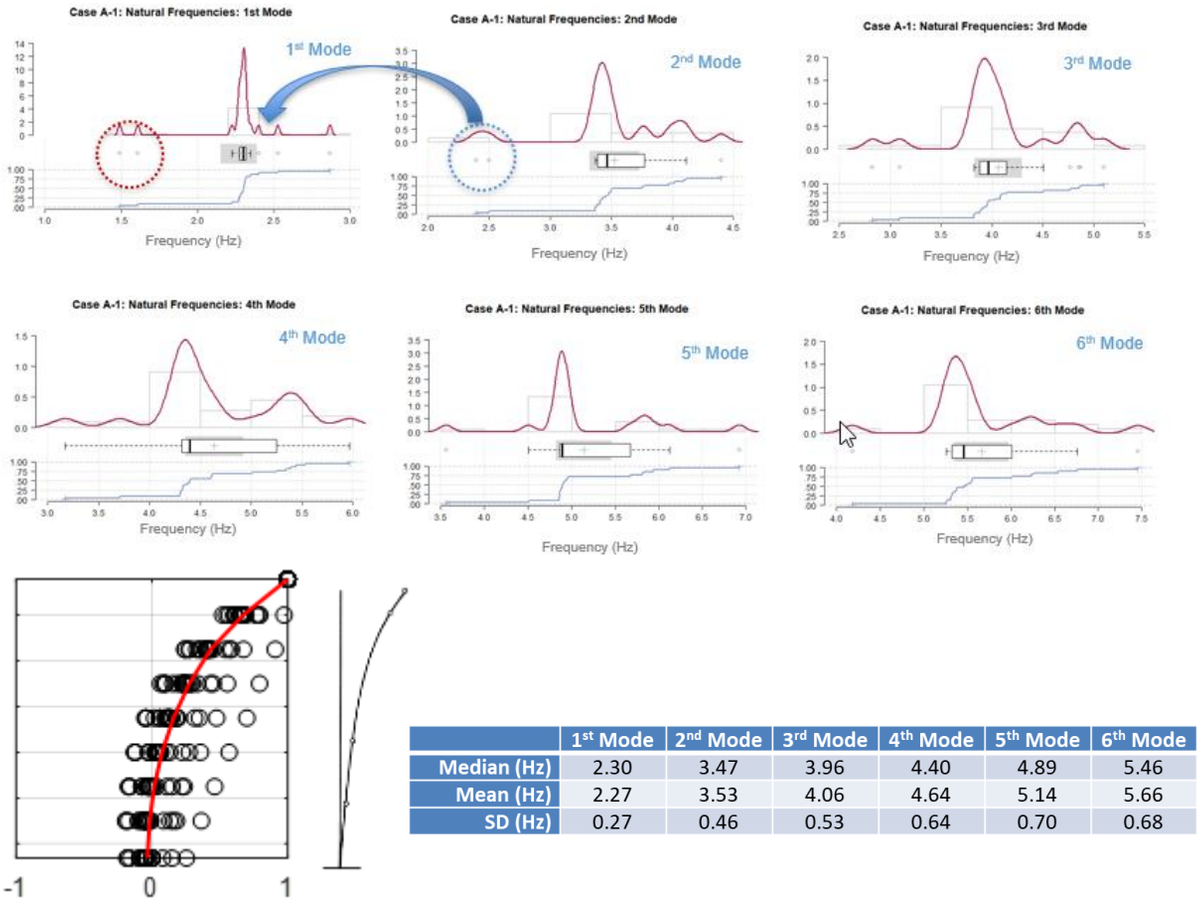

	1st Mode	2nd Mode	3rd Mode	4th Mode	5th Mode	6th Mode
Median (Hz)	2.30	3.47	3.96	4.40	4.89	5.46
Mean (Hz)	2.27	3.53	4.06	4.64	5.14	5.66
SD (Hz)	0.27	0.46	0.53	0.64	0.70	0.68

Figure 2. Distribution of results for the first mode shape and six natural frequencies obtained by the contributors.

Then, the linear dynamic analyses were performed for a synthetic harmonic excitation to be applied at the dam crest. This harmonic excitation was developed based on the results of the eccentric-mass vibration generator (EMVG) test performed at Pine Flat Dam in 1971 (Rea, Liaw & Chopra, 1972). The synthetic EMVG load signal was subjected to Hann windowing function to avoid numerical artifacts. In the simulations, the amplitude of the load record corresponded to 35.4 kN with the first fundamental frequency of 3.47 Hz, obtained from the experiments, and the viscous damping of 2%.

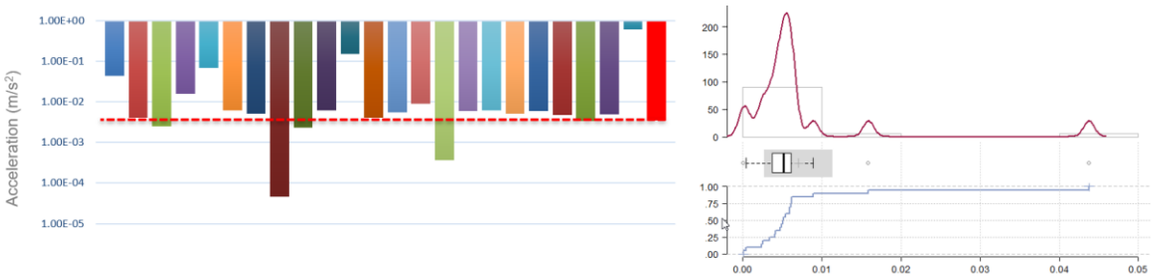

	Point C
Median Peak Acc. (m/s²)	5.12×10^{-3}
Mean Peak Acc. (m/s²)	7.05×10^{-3}
SD Peak Acc. (m/s²)	9.24×10^{-3}

Figure 3. Results at the crest of the dam provided by Contributors compared with EMVG test data.

Most of the Contributors obtained similar results from the EMVG simulation, except for a few outliers, where the median of the predicted peak acceleration was 5.1 mm/s^2 (Figure 3). This is relatively close to the measured peak acceleration of the crest of 3.5 mm/s^2. The relatively small discrepancy could be due to slightly higher damping measured in the test than used in the analyses. The prediction of the calculated peak displacement showed lower agreement with the measured displacements. It should, however, be noted that the displacements obtained from this excitation are quite small and could be limited by the accuracy of the sensors, thereby resulting in larger uncertainties.

2.2 *Case B – Foundation analysis using impulsive loads*

The purpose of the Case B study was to verify commonly-used nonreflecting boundary conditions in an analysis of a wave propagation in an elastic foundation block, and to investigate the effect of foundation size for the impulsive stress records. Foundation blocks (one with dimension of 700 x 122 m, and one with dimensions of 3700 m x 122 m) was considered in simulations for a high- and low-frequency shear stress pulses applied at the base of the block model with zero viscous damping. Each Contributor was asked to select a nonreflecting boundary condition to be applied to the sides and base of the model.

Contributors provided time-histories of velocity results at selected points "a" through "g" along the top surface of the block, where point "a" is at the center, and "g" is at the side edge of the block. The ideal results would perfectly match the theoretical record obtained for a semi-infinite half-space for the same applied impulse excitation. The left and right plots in Figure 4 show the results in time and frequency domain for the analysis conducted with "free-field" and "nonreflecting" boundary conditions, respectively.

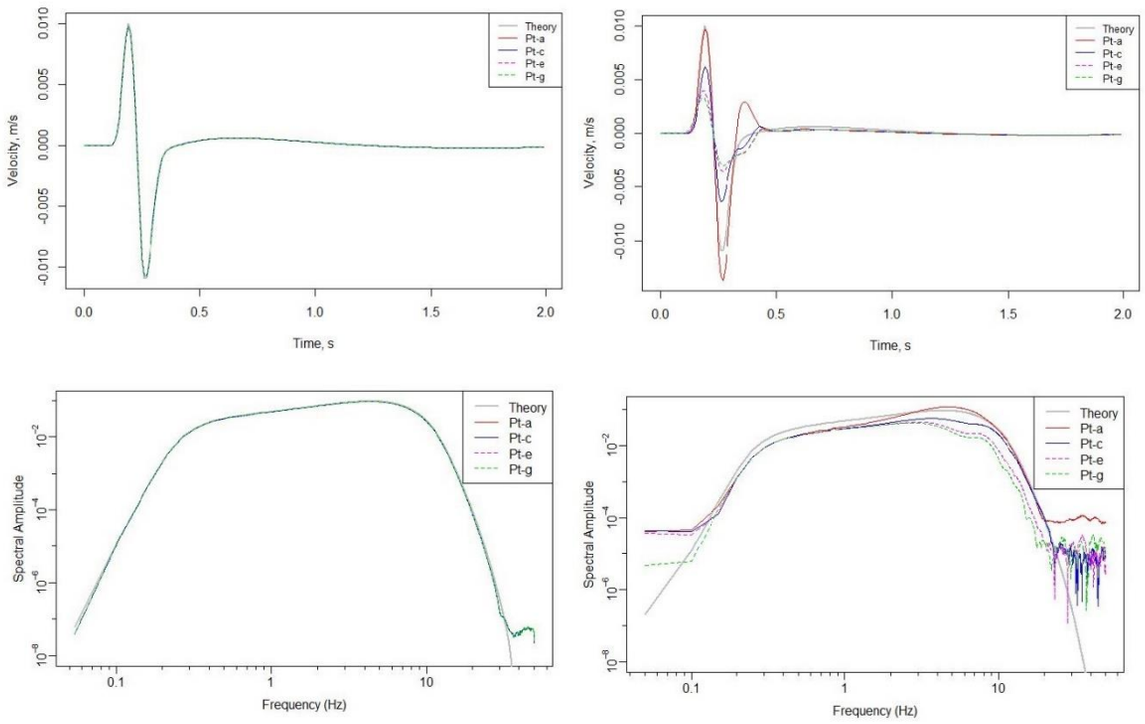

Figure 4. The results in time and frequency domain obtained for "free-field" (left) and "nonreflecting" (right) boundary conditions.

Very good agreement with the theoretical solution is observed for the results provided by Contributors using "free-field" boundary conditions (see Figure 5, left). The uniformly applied wave at the block base remains uniform at the top of the foundation block as expected. For "nonreflecting" boundary conditions, however, the relatively good agreement with the theoretical solution is observed only at the center of the foundation block, with significant differences away from the center (affected by the boundary conditions) (see Figure 5, right). In addition, the size of the foundation in the horizontal direction had very limited influence on the results, especially when the free-field boundary conditions

were implemented. Similar observations were made for the simulations with the high- and low-frequency pulse excitation.

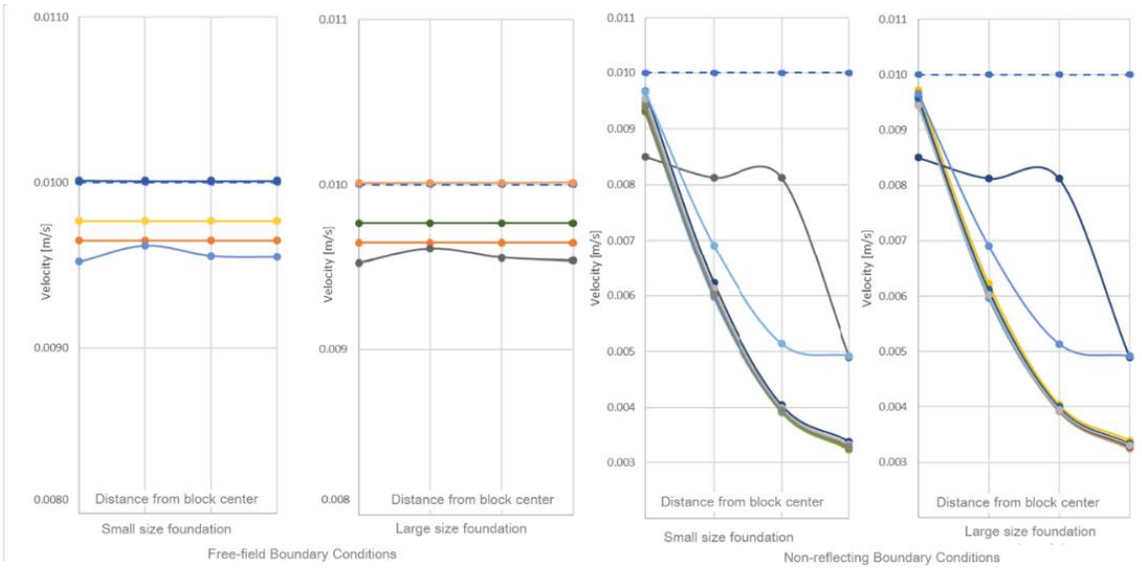

Figure 5. Distribution of horizontal peak velocities at the upper face of the foundation block for small and large size foundation blocks computed for the low-frequency pulse. Results for the free-field boundary conditions (left two plots) and the nonreflecting boundary conditions (right two plots) are compared with the theoretical solution (blue dashed line).

2.3 *Case C – Dynamic analysis using impulsive loads*

In Case C, the analysis for the base model configuration was conducted with the material properties and the load conditions defined for the foundation block in Case B.

Analysis results show a significant reduction of the velocity amplitude at the dam base (point "a") compared with the corresponding velocity amplitude at the free-surface (point "c") (Figures 6 and 7). Also, the reservoir presence in the model had a limited influence on the velocity amplitude at the dam heel, but a more significant difference was observed at the dam crest.

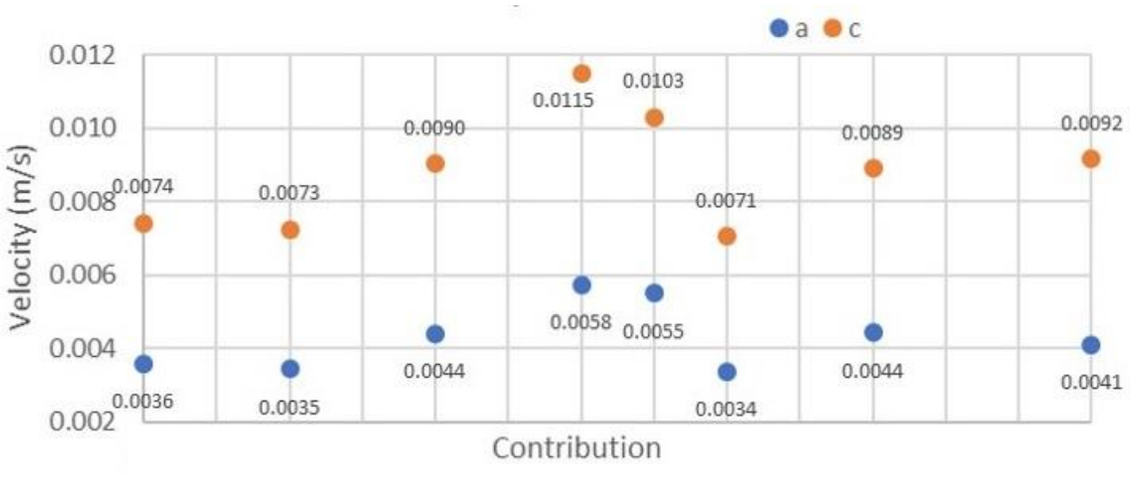

Figure 6. Maximum peak velocity at point "a" (center of the dam base) and point "c" (free surface) for a high frequency pulse submitted by eight Contributors.

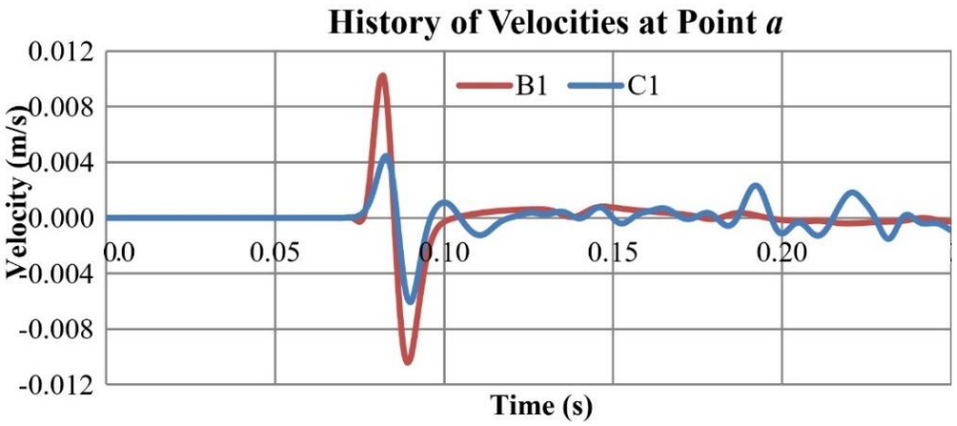

Figure 7. Comparison of velocity time histories at the center of the foundation block (point "a") for Case B (without dam) and Case C (with the dam and the reservoir presence) for a high frequency pulse excitation.

2.4 *Cases D & F – Mass and massless foundation analysis for various reservoir levels*

Linear dynamic analysis of the dam-reservoir-foundation system (base model configuration) was conducted in Case D considering three reservoir water levels (winter, summer, and normal levels differing from each other by about 10 m). The input load was based on one horizontal component of the Taft earthquake record (peak acceleration of 0.18 g), which was assumed to represent the ground motion at the free surface of an elastic half-space. For input, Contributors could use either an acceleration record which had been deconvolved to the base of the foundation, or a stress record which was computed from the integrated free-surface acceleration. In the linear elastic analyses, the mass foundation was considered with 2% viscous damping assumed for both the dam and the foundation. Contributors were requested to select the size and the type of finite elements, the fluid-structure interaction approach, and the relevant nonreflecting boundary conditions.

Different boundary conditions and computational approaches were used, including the free-field boundary condition, nonreflecting (absorbing) boundaries, infinite elements, perfectly matched layers (PML), and the domain reduction method. Figure 8 shows an acceleration and displacement comparison among results for the winter reservoir level (case D-1). Results from Contributors who used the free-field boundary conditions generally showed good agreement, while results from those who did not use the free-field boundary conditions generally showed greater variability.

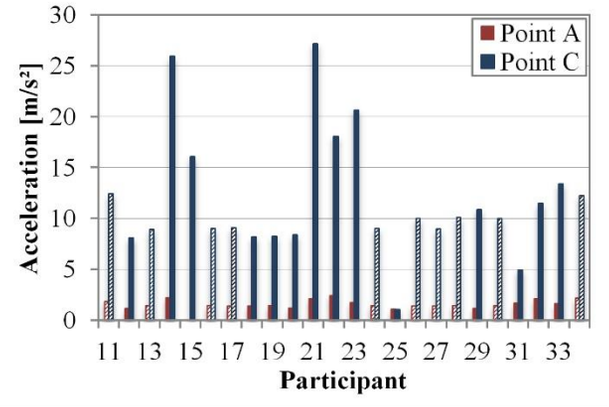

(a) Acceleration at dam heel (point A) and dam crest (point C)

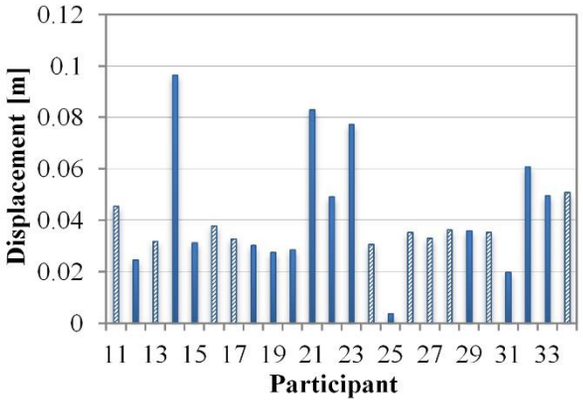

(b) Relative displacement between the dam crest and the dam heel

Figure 8. Results of analysis for the Taft earthquake record and winter reservoir water level (dashed histograms indicate contributors using free-field boundary conditions).

The model for Case F is similar to the one described for Case D, except that the massless approach is adopted for the foundation block. Linear dynamic analysis is conducted, as in Case D, considering

the three reservoir water levels. The horizontal Taft earthquake acceleration record (free-surface) is applied at the free surface of the foundation. In the analysis, the mass of foundation is assumed equal to zero, and a 2% viscous damping is assumed for the dam. The results obtained from models with massless foundation and winter reservoir level (Case F-1), showed in Figure 9, are unexpectedly quite variable in terms of accelerations and displacements.

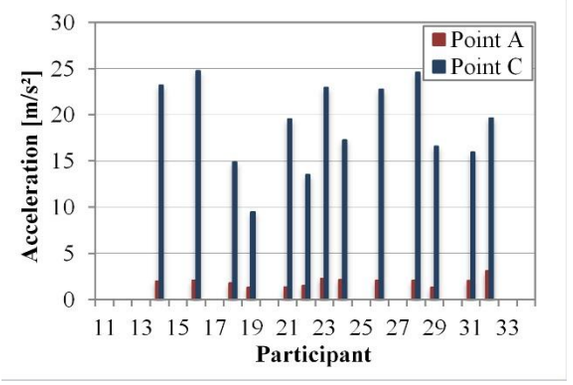

(a) Acceleration at dam heel (Point A) and dam crest (Point C)

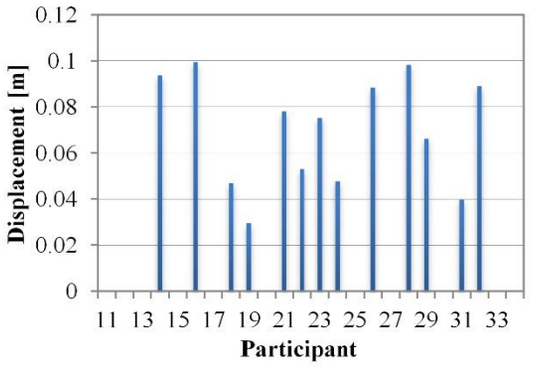

(b) Relative displacement between the dam crest and dam heel

Figure 9. Results of massless foundation analysis for Taft earthquake record and winter reservoir level.

The analysis results for the model with a massless foundation show larger acceleration and displacement amplitudes compared to the results obtained from similar analyses with mass type foundations (Figures 10 and 11).

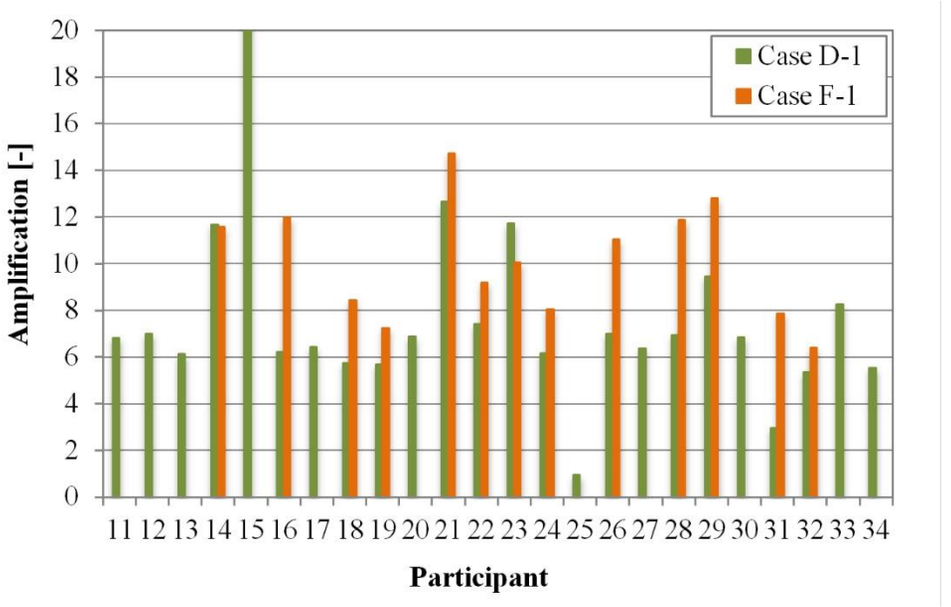

Figure 10. Comparison between Case D-1 and Case F-1 for winter reservoir level conditions: amplification of acceleration at the dam crest.

Cases D and F show the dependency on water elevation of the computed net displacements and accelerations between the crest and heel of the dam. Results are shown in Figure 11. In general, the highest water level (WRWL 290) produces the lowest net displacement and acceleration, however, this reduction is more apparent for accelerations (30-40%) than for displacements (7-27%). The massless foundation (Case F) produces about a factor of 2 larger accelerations at all water elevations than does a foundation with mass (Case D). For displacements, the massless foundation also produces

about a factor of 2 amplification compared to the foundation with mass, except for the highest water level, where the factor is about 1.5. To combine results, displacement and acceleration values are computed for each Contributor's time-histories at Points C and A (crest and heel - see Figure 1), using a mean amplitude = (max – min)/2. Next the net displacement and acceleration for each Contributor are computed by subtracting the mean amplitude at Point A from that of Point C. Finally, the median of the net amplitudes over all contributors is computed and plotted.

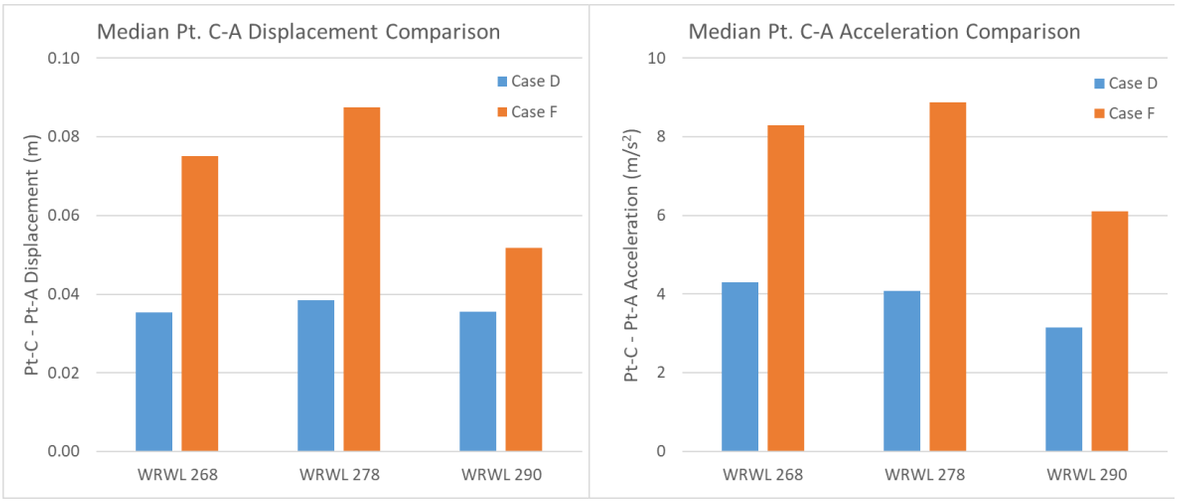

Figure 11. Net displacements (left plot) and accelerations (right plot) for water levels 268, 278, and 290 (winter, summer, and normal conditions, respectively) for Cases D (blue) and F (orange). See text for discussion.

2.5 *Case E –Dynamic analysis with nonlinear concrete material*

Case E is an extension of Case D with considered nonlinear concrete material properties. Moreover, the analyses are performed for two different dynamic input load records (i.e., the deconvolved Taft earthquake record in a form of an acceleration or stress time history (Case E-1), and an artificially generated intensifying record called Endurance Time Acceleration Function (ETAF, Case E-2). The analysis of the base model was conducted for the winter reservoir level, dynamic excitation applied at the base of the foundation, and 2% viscous damping.

In general, the Contributors adopted different nonlinear damage models. For the Taft record, Contributors had good agreement in predicting relative crest displacement and hydrodynamic pressure at the heel, as shown in Figure 12(a) and 12(b) (one may notice some outliers among data). Figure 12(c) shows variation of the acceleration response as a ratio of amplitude spectrum of the crest point with respect to heel. At the dam fundamental period, this ratio is 10-20 times. More importantly, the damage at the dam base (i.e., dam-foundation interface) varies from 0 to 35% of base length (with the median of 4%), as shown in Figure 12(d). One may note that the damage index (DI) is defined as a ratio of base crack length to the length of the dam base. The DI is sensitive to the selected concrete damage model and mesh density. Study of the dam model and Taft record revealed the potential damage zones were located at the dam heel and at the downstream face next to neck slope change, as shown in Figure 12(e).

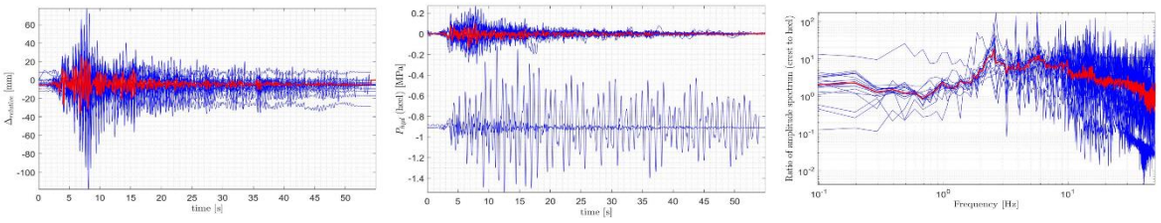

(a) Crest relative displacement (b) Heel hydrodynamic pressure (c) Ratio of amplitude spectrum

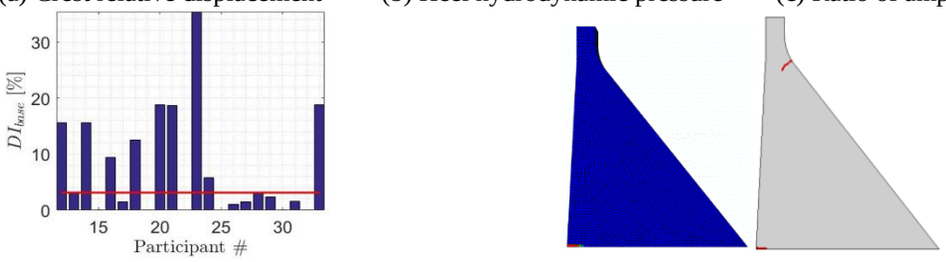

(d) Damage index (e) Damage profile at the end of earthquake

Figure 12. Results of nonlinear analysis under Taft earthquake record (Case E-1 for winter reservoir level).

For ETAF record, significant differences exist in all the predicted structural responses (i.e., displacements, hydrodynamic pressure, and DI). Figure 13(a) presents the variation of relative crest displacement for 15 seconds of applied ETAF record. Although the median (red) curve shows a total of about 400 mm displacement at t = 15 sec, some models predict a displacement as high as 4,800 mm. There is a similar conclusion on potential failure modes and the anticipated failure time. Figure 13(b) presents the damage map for two selected models. The right map shows the damage profile at t = 15 sec (failure time), while the left map predicts the failure to occur at t = 2 sec. Moreover, increasing the intensity of applied dynamic excitation shifts the response to nonlinear phase and, subsequently, increases the uncertainty. Finally, as observed in Figure 13(c), the length-based DI (ratio of base crack to base length) is completely different than the area-based DI (ratio of damage area to total dam area). The length-based DI appears more stable because it is less sensitive to mesh size. For very fine meshes, it is recommended that the area-based DI not be used.

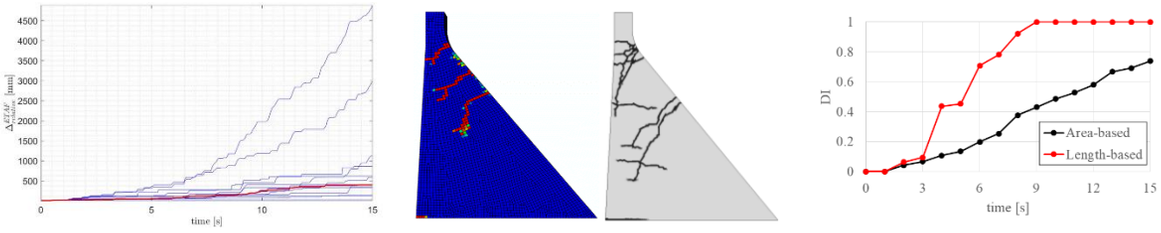

(a) Crest relative displacement (b) Damage profile at 2 and 15 sec (c) Different DI definitions

Figure 13. Results of nonlinear analysis under ETAF acceleration (Case E-2).

Compared to the results from Case D, the uncertainty in nonlinear analysis is larger than for linear elastic models. Furthermore, the global response (e.g., displacement) is less uncertain than the local response (e.g., damage index). This implies that one may predict a (relatively) good nonlinear displacement, while a damage prediction might be still at a low level.

3 SUMMARY AND CONCLUSIONS

3.1 *Summary*

The 2019 ICOLD Benchmark Workshop is a step in developing a forum where:

- The analyst can verify the performance and behavior of modeling software before using it in a seismic analysis of concrete dams.
- The software developer can verify and validate modeling software features and the accuracy of the software using the results of the benchmark studies.
- The researcher can further expand and investigate topics presented in the benchmark workshop.
- Dam owners can build confidence in analysis results obtained using modeling software that has been verified with the benchmark study cases.

In comparing various results for different computational models, the most significant factor affecting the misfit between computed and theoretical results is the use of the free-field boundary condition. This effect primarily results from reflections generated at the side boundaries as the amplitude of the incident wave is artificially reduced to zero by using only the absorbing boundary condition.

3.2 *Conclusions*

The investigations conducted for Theme A of the 2019 ICOLD Benchmark Workshops led to the following conclusions:

- Computation models need to be verified before they are used in any analysis of concrete dams.
- A coordinated and systematic verification process for seismic analyses of concrete dams needs to be establish throughout the engineering community.

4 REFERENCES

Bureau of Reclamation. 2018.: Evaluation of numerical models and input parameters in the analysis of concrete dams. Result summary of the USSD Workshop, Miami, May 3, 2018. DSO-19-13 report https://www.usbr.gov/ssle/damsafety/TechDev/DSOTechDev/DSO-2019-13.pdf

Salamon J., Hariri-Ardebili M.A., Malm R., Wood C., Faggiani G. 2019. Seismic analysis of Pine Flat Concrete Dam. ICOLD 15th International Benchmark Workshop on Numerical Analysis of Dams, Theme A: Seismic Analysis of Pine Flat Concrete Dam. International Committee on Large Dams, March 18, 2019.

ICOLD. 2019. 15th International Benchmark Workshop on Numerical Analysis of Dams, Theme A: Seismic Analysis of Pine Flat Concrete Dam. International Committee on Large Dams, November 2019.

Rea D., Liaw, C.Y. & Chopra, A.K. 1972. Dynamic properties of Pine Flat Dam. Report No. UCB/EERC-72/7, December 1972.